Materials Science of Carbon Nanotubes: Fabrication, Integration, and Properties of Macroscopic Structures of Carbon Nanotubes

OTTO ZHOU,* HIDEO SHIMODA, BO GAO, SOOJIN OH, LES FLEMING, AND GUOZHEN YUE

Curriculum in Applied and Materials Sciences, and Department of Physics and Astronomy, University of North Carolina, Chapel Hill, North Carolina 27599

Received April 2, 2002

ABSTRACT

In this Account, we summarize some of our recent studies on the materials properties of the carbon nanotubes (CNTs). The focus is on single-wall carbon nanotubes (SWNTs). We describe experiments on synthesis of SWNTs with controlled molecular structures and assembly of functional *macroscopic* structures. In addition, we present results on the electron field emission properties of macroscopic CNT cathodes.

1. Introduction

The last 10 years has been an exciting time for the field of carbon materials. The discoveries of fullerenes[1,2] and carbon nanotubes (CNTs)[3] have attracted the attention and imagination of many researchers worldwide. Tremendous amounts of research and development efforts have been devoted to the studies of these new carbon allotropes. The findings have significantly extended our understanding of the fundamental science at the nanometer scale and created the opportunities for future technologies. The research in fullerenes chemistry has led to the discovery of molecular superconductors with a record high transition temperature.[4] Potential applications of CNTs in vacuum electronics, nanodevices, and energy storage have been demonstrated at the prototype level.[5]

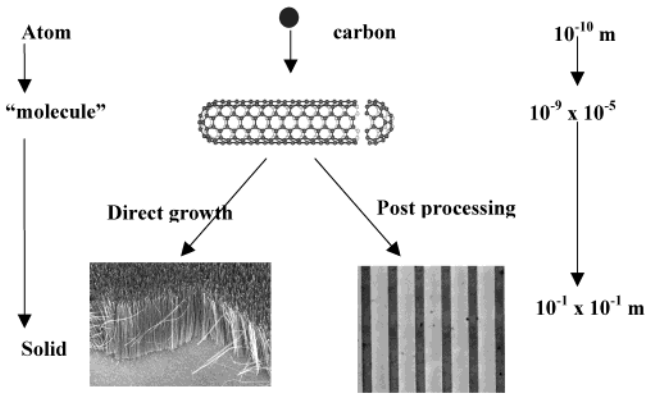

FIGURE 1. Functional *macroscopic* structures of CNTs can be fabricated by either direct growth via chemical vapor deposition or postdeposition using preformed CNTs. In either approach, fabrication of homogeneous materials requires control of not only the molecular structures of the individual building blocks but also the higher level architectures by which the molecules assemble.

From the materials point of view, the nature of CNTs differs significantly from that of the fullerenes. C_{60}, as a molecule, can be made with precise and uniform composition and a molecular structure that is essentially defect-free.[6,7] Functional C_{60} solids such as single crystals and epitaxial films can be readily fabricated. The case of CNTs is more complicated. A CNT is not a well-defined molecule. It comes with different structure, weight, dimension, and, as a result, different properties. The variations in the "molecular" architecture in principle provide an additional materials design parameter. However, the polydispersity also leads to nonuniform and unpredictable properties. Fabrication of homogeneous materials requires control of not only the individual building blocks but also the higher level architecture by which the "molecules" assemble (Figure 1). Contrary to the ideal model of perfect cylindrical graphene structures, point defects, dislocations, and impurities are abundant, which significantly affect the properties of the CNTs. Due to these complications, fabrication of functional macroscopic CNT structures that can fully utilize the novel properties of the individual CNTs is challenging.

In this Account, we summarize some recent works carried out in our group on the materials science aspects of the carbon nanotubes. We begin by describing some experiments on controlling the molecular structures of single-wall carbon nanotubes (SWNTs). We then discuss methods to assemble *macroscopic* structures of CNTs into hierarchical structures. In the last section, we present results on the electron field emission properties of macroscopic CNT cathodes.

2. Fabrication and Processing of SWNTs

2.1. Synthesis. Carbon nanotubes with different structure and morphology can now be produced in laboratory

Otto Zhou received his Ph.D. degree in materials science from the University of Pennsylvania in 1992. He was a postdoctoral member of the technical staff at the Bell Labs and a visiting scientist at the NEC Fundamental Research Lab before joining UNC Chapel Hill in 1996. He is currently Associate Professor of Materials Science and Physics.

Hideo Shimoda received his Ph.D. degree in materials science from Japan Advanced Institute of Science and Technology in 1999. He is currently a research assistant professor at UNC.

Bo Gao received his Ph.D. degree in materials science from UNC Chapel Hill in 2001. He is now a scientist at Applied Nanotechnologies, Inc.

Soojin Oh received her M.S. degree in physics from Pohang University of Science and Technology in Korea in 1996 and is now a Ph.D. student in the materials science program at UNC.

Les Fleming received his B.S. degree from Florida State and is currently a Ph.D. student in physics at UNC.

GuoZhen Yue received his Ph.D. degree from the Chinese Academy of Science in 1998. He is currently a research assistant professor at UNC.

* Corresponding author. E-mail: zhou@physics.unc.edu.

10.1021/ar010162f CCC: $22.00 © 2002 American Chemical Society
Published on Web 11/27/2002

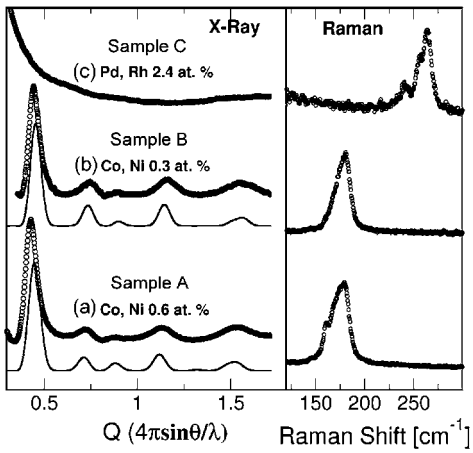

FIGURE 2. (Left) Experimental and simulated X-ray diffraction patterns of SWNTs made using different catalysts. The average tube diameters of samples A and B are 1.40 and 1.32 nm, respectively. (Right) The Raman spectra from the same samples collected using 514-nm laser light. The average peak positions of the SWNT breathing mode are 172, 175, and 258 cm^{-1} for samples A, B, and C, respectively. Breathing mode at 258 cm^{-1} in sample C corresponds to an average tube diameter of 0.85 nm.

quantities by arc discharge,[8,9] laser ablation,[10] and chemical vapor deposition (CVD)[11−14] techniques. Materials produced by the first two methods are in the forms of porous membranes and powders that require further processing. CNTs can be grown directly on substrates by the CVD process. Considerable efforts have been directed toward synthesizing SWNTs with uniform and variable size[15−19] and, more importantly, electronic properties. Progress, however, has been slow due to the lack of understanding of the growth mechanism and the similarities in the formation energies. It has been found experimentally that the SWNTs produced by the laser ablation method have a random distribution in chirality.[20,21] Bulk materials comprise one-third metallic and two-thirds semiconducting nanotubes.[22] Here we present results showing that the diameter and the electronic properties of the SWNTs can be varied by choosing different catalysts used in the laser ablation process.

We synthesized SWNTs using Rh and Pd catalysts instead of the common Ni/Co system. Rh and Pd have higher melting temperatures compared to Ni and Co and have finite solubility of C. In addition, they are nonmagnetic, making the materials easier to characterize. The synthesis procedure is similar to that previously described.[19] All of the samples are 10% ^{13}C-enriched. The targets are ablated by a Nd:YAG laser in an Ar-filled chamber. The structure and electronic properties are characterized by X-ray, Raman, and nuclear magnetic resonance (NMR) techniques.

Figure 2 compares the SWNTs synthesized by using the Ni/Co and Rh/Pd catalysts. X-ray diffraction and simulations[23] show that the average diameter of the nanotubes made by the Ni/Co samples is between 1.3 and 1.4 nm, depending on the catalyst concentration, consistent with the previous results.[10] The nanotubes made by using the Rh/Pd catalyst show no Bragg diffraction peaks, indicating a smaller bundle diameter and/or packing disorder. The Raman-active SWNT radial breathing mode is shifted from ∼172 to 258 cm^{-1} when Rh and Pd are used as the catalysts. Using the relationship between the vibration frequency and the diameter of the SWNTs,[24] the average diameter of SWNTs made using Rh/Pd is estimated to be 0.85 nm.

The NMR technique is used to investigate the electronic properties of the SWNTs.[19,22] Care is taken to remove the Ni/Co catalysts so that the signals are not obscured by the local magnetic field. ^{13}C spin−lattice relaxation measurements show that the density of states at the Fermi level increases with decreasing nanotube diameter. In addition, the mass ratio between the metallic and semiconducting SWNTs changes with the catalysts used. The samples produced by the Ni/Co catalysts are composed of one-third metallic and two-thirds semiconducting SWNTs, consistent with a random chirality distribution. The percentage of the metallic tubes increases to ∼70% when 1.2 at. % each of Rh/Pd is used as the catalyst.

The reason for the smaller diameter SWNTs produced by using Rh/Pd catalysts is not clear. We attribute this to the difference in the melting temperature between the Rh/Pd and Ni/Co systems. The former has a much higher melting point. At the same furnace temperature (1100 °C), the degree of supercooling is much larger for the Rh/Pd system than for the Ni/Co system. As a result, the critical radius for nucleation, which is related to the surface energy, latent heat, and degree of supercooling, is smaller for the former.[25] On the basis of the current understanding of a vapor−liquid−solid transformation (VLS) model for nanotube formation, this will lead to smaller diameter nanotubes.

2.2. Purification. As-synthesized carbon nanotube materials contain significant amounts of impurities, including amorphous carbon (α-C), graphitic particles, and metal catalysts. The purification schemes that have been developed usually take advantage of the differences in the aspect ratio[26] and oxidation rate[27,28] between the nanotubes and the impurities. Although the majority of the impurity phases can be eliminated by a combination of filtration and oxidation treatments, these processes also damage the structural integrity of the nanotubes by creating defects on the graphene shells.[29]

A combination of hydrogen peroxide (H_2O_2) reflux and filtration[30] is an effective way to remove most of the impurities without causing much damage to the nanotube compared to, for example, sonication in more potent acid such as nitric acid.[29] In this process, raw materials (Figure 3A) are first refluxed in H_2O_2. α-C is preferentially reacted with H_2O_2. The residual (∼30 wt %) is rinsed first in CS_2 to remove C_{60} and then in methanol. At this stage, the material contains mostly SWNT bundles and catalysts protected by graphitic shells (Figure 3B). They are then filtered through 0.8−2-μm pore-size membranes. A significant fraction of the nanoparticles and magnetic catalysts can be removed by repeating the filtration process several times until the liquid passing through the filter is clear. The purity of the final product can reach over 95% (Figure 3C,D), although the precise value is difficult to

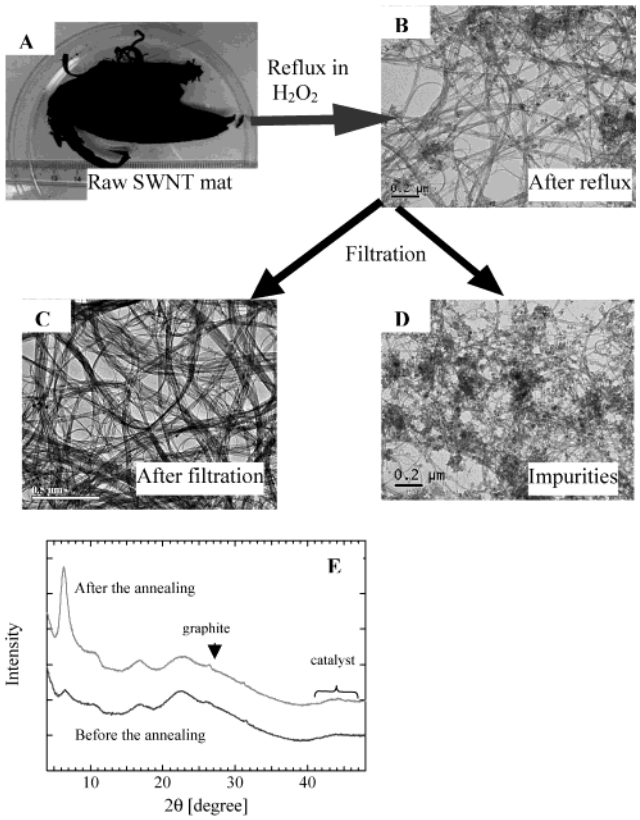

FIGURE 3. (A−D) Representative micrographs of SWNTs at different stages of the purification process. (E) Powder X-ray diffraction patterns of the purified SWNT bundles before and after annealing. Note that there is very little graphite or catalysts left in the purified sample.

determine. After purification, the SWNT bundles can be recrystallized by annealing in a vacuum at 800−1000 °C for a short time. The end product is no longer magnetic: the bundles cannot be moved by a magnet and no Ni/Co Bragg peaks are present in the X-ray diffraction pattern (Figure 3E). The purified materials show a strong electron spin resonance (ESR) signal from the conduction electrons and a narrow ^{13}C NMR peak of the SWNTs.

2.3. Opening and Closing the SWNTs Tips. Pristine SWNTs have large aspect ratios (10^3−10^4) and closed ends, which prevents the diffusion of the guest species into the interior spaces of the nanotubes. It has been shown, mostly through TEM measurements, that the nanotubes can be fractured and shortened by techniques such as ball-milling,[31,32] mechanical cutting,[33] and chemical etching.[34−36] For macroscopic measurements of the open-end nanotubes, most of the nanotubes need to be opened and have similar lengths. These characteristics have not been demonstrated by the ball-milling and mechanical cutting processes. Here we present results from both local and macroscopic experiments to demonstrate that the SWNTs can be opened and shortened uniformly by chemical etching. Furthermore, the opened SWNTs can again be closed.

Upon sonication in strong acid, oxidation of the nanotubes is believed to initiate from the sidewall defects

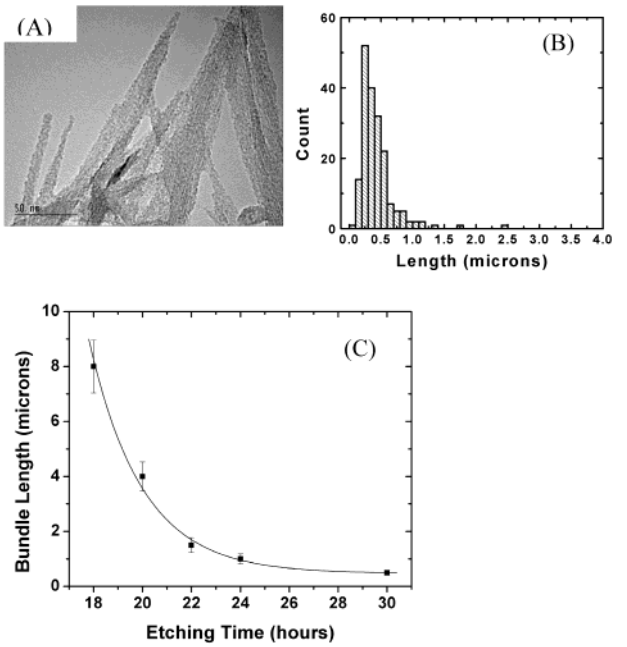

FIGURE 4. (A) TEM micrograph showing that tips of the etched SWNT bundles have a conical geometry. (B) Length distribution of the SWNTs etched for 30 h. (C) Experimentally observed relationship between the average bundle length and the processing time.

on the bundle surfaces and the tips, where the reactivity is higher. The reaction then propagates throughout the bundles. This defect-assisted mechanism is supported by the structure of the etched tubes and the overall weight change. TEM micrographs show that the tips of the shortened SWNT bundles are mostly tapered (Figure 4A), which is distinctly different from the case with those made by mechanical cutting[33] and ball-milling.[31] Experimentally, we found a weight loss of 70% when the purified SWNTs ($L > 10\ \mu$m) were etched to 0.5 μm average length. This is significantly higher than what is expected if reaction occurs only at the ends. In addition, the effectiveness and the rate of the etching process depend highly on how the starting materials are synthesized. For SWNTs synthesized by the laser ablation method in our laboratory, the averaged bundle length can be reduced to ∼0.5 μm with a narrow distribution after 30 h of sonication in strong acid (Figure 4B 4C). After etching, the nanotubes are still in the form of bundles.

Careful examinations by HRTEM reveal that the SWNT tips are open after etching (Figure 5A). In some cases, disordered structures are observed at the tips which are attributed to functional groups that terminate the broken carbon bonds (Figure 5B). No closed ends were observed in all the shortened SWNTs that we could clearly image, even when the samples were vacuum-annealed below 400 °C. The open ends can be again closed by vacuum annealing at temperatures above 500 °C. Figure 5C shows a HRTEM image of the tips of the individual SWNTs after annealing at 800 °C under 10^{-6} Torr dynamic vacuum. All the observed tips are closed and apparently well graphitized. However, instead of the ideal hemispherical geometry, they are closer to polygons, as often observed in the MWNTs.

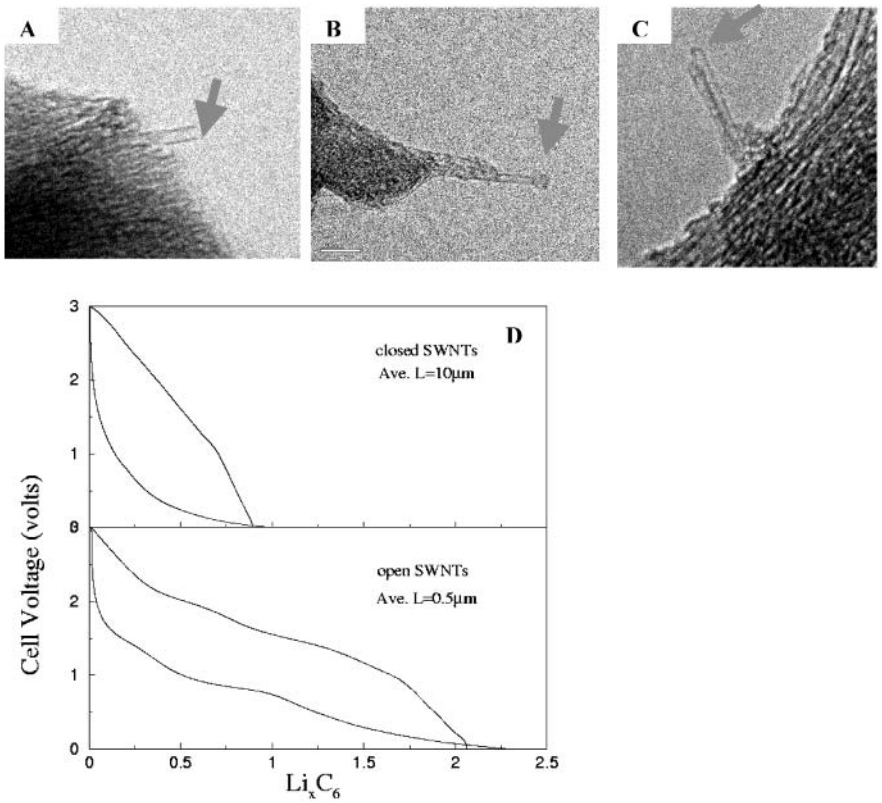

FIGURE 5. High-resolution TEM micrographs showing that the tips of the etched SWNTs are either (A) open or (B) terminated by large chemical groups. (C) After annealing in a vacuum at 800 °C, the ends are closed again. (D) Second cycle charge−discharge data (cell voltage versus Li concentration) obtained from purified SWNTs and samples after chemical etching. The data were collected at 50 mA/g rate.

Electrochemistry and NMR studies[36] show a drastic enhancement of the specific storage capacity of Li in the open-end SWNTs. Figure 5D compares the reversible Li storage capacity in the closed and opened SWNTs measured under otherwise the same conditions. For close-end SWNTs, a reversible capacity of LiC_6 is observed which is similar to the value for graphite and consistent with Li occupying only the interstitial sites within the SWNT bundles.[37,38] For open-end SWNTs, the specific Li storage capacity increases to LiC_3.[36,39] The increase in capacity is explained by diffusion of Li^+ into the interior spaces of the SWNTs which are inaccessible in the close-end tubes.

2.4. Tuning the Electronic Properties. Charge transfer is an effective method to modify the electronic properties of the carbon nanotubes. Similar to graphite, both electron donors and acceptors can be readily inserted into the interstitial sites of the SWNT bundles or the interlayer spacing of the MWNTs via redox reactions. Charge transfer leads to significant changes in the properties of the host materials.[36,40−43] ^{13}C nuclear spin−lattice relaxation experiments show that all the SWNTs become metallic upon lithium intercalation. As shown in Figure 6A, the saturation recovery curve of the pristine SWNT sample can be fit with a double-exponential function.[19] The fast-relaxing component is attributed to the metallic SWNTs, while the slow-relaxing component is attributed to the semiconducting SWNTs. The lithium-intercalated samples can be fitted with a single-exponential function, indicating that all the SWNTs in the sample have the same average electronic properties. The relaxation time decreases with increasing Li/C ratio, indicating an increase of the density of states at the Fermi level.[36]

Furthermore, in situ photoemission spectroscopy experiments[44,45] show that the electron work function of the CNTs can be substantially reduced by intercalation of electron donors such as cesium (Figure 6B). The pristine SWNT bundles have a work function of 4.8 eV, similar to that of graphite. Upon exposure to Cs vapor in a controlled environment, the work function decreases with increasing exposure time. A distinct Fermi edge is observed in the Cs-intercalated SWNTs.[44] Electron field emission measurement of the intercalated SWNTs shows that the threshold field for emission decreases with increasing Cs exposure time,[46] consistent with reduction of the electronic work function due to Cs intercalation.

3. Integration

3.1. Self-Assembly. Self-assembly is often a preferred process to assemble micro- and nanoscale objects into ordered *macroscopic* structures.[47] It has been utilized to produce functional materials such as photonic crystals, nanocomposites, and ordered DNA structures. We have recently shown that functional hierarchical structures of CNTs with long-range ordering can be readily fabricated at room temperature via self-assembly.[48] This process has several advantages over the CVD and other postprocessing methods.

In this process, SWNT bundles are first rendered hydrophilic and are dispersed in deionized water at a

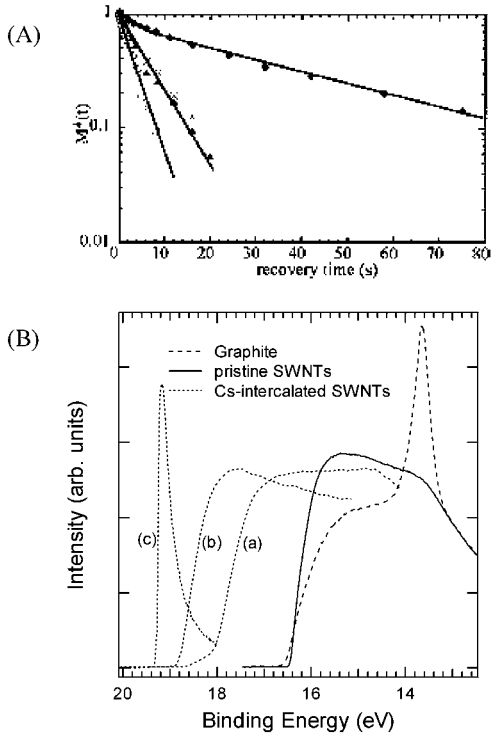

FIGURE 6. (A) ^{13}C nuclear spin−lattice relaxation (NSLR) curves. The curve from the pristine sample (◆) can be fitted with a double-exponential function. The fast-relaxing component is attributed to the metallic SWNTs, while the slow-relaxing component is attributed to the semiconducting SWNTs. The NSLR curves of the LiC_6 (▲) and LiC_3 (etched SWNT, ○) samples can be fitted with a single-exponential function with the respective T_1 of 6.5 and 3.2 s, respectively. (B) Photoemission spectra around the secondary electron threshold regions of graphite and the pristine and Cs-intercalated SWNT bundles. (a), (b), and (c) correspond to different Cs concentrations. (Data taken from ref 44.)

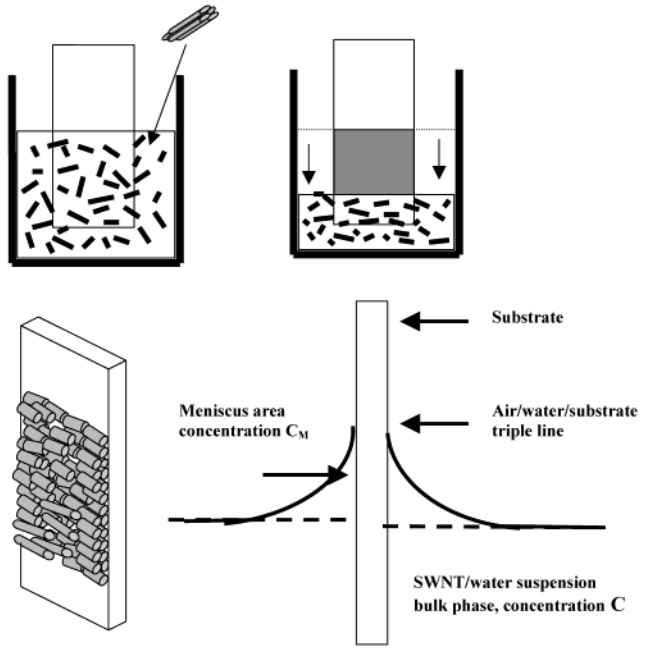

FIGURE 7. Schematic illustration of the self-assembly process. Etched SWNTs were dispersed in deionized water to form a stable suspension into which a hydrophilic glass slide was vertically immersed. With gradual evaporation of the water, the SWNT bundles self-assembled on the glass substrate around the air/water/substrate triple line. As the triple line progressed downward, a continuous SWNT film was formed on the substrate.

concentration of 0.5−1 g/L. A clean hydrophilic substrate such as glass is immersed vertically into the suspension (Figure 7). The nanotubes deposit on the substrate along the air/liquid/substrate triple line. A continuous SWNT film forms on the substrate as the triple line progresses downward. The films are smooth and have stepwise sharp edges that are straight at the substrate/film interface. Electron microscopy studies reveal that the SWNT bundles are orientationally ordered, with their longitudinal axes lying on the substrate surface and along the air/water/substrate triple line direction (Figure 8). Similar to the structure of nematic liquid crystals, there is no translational ordering. Under a cross-polarized optical microscope, the *macroscopic* SWNT films show birefringence, with extinction at 0° (nanotube alignment direction parallel to the polarization direction) and 90° (Figure 8B) and maximum transparency at 45° over the entire surface area (Figure 8C).

The hydrophilic nanotubes deposit only on the *hydrophilic*, not on the *hydrophobic*, surface. This selectivity enables the fabrication of patterned structures by controlling the functionality of the supporting surface. As demonstrated in Figure 8D, periodic structures with a characteristic dimension of 100 μm or lower can be readily deposited on glass substrates at room temperature. The well-defined structures can be utilized as, for example, the basic emission pixels for field emission display (FED). The efficient room-temperature deposition process is attractive compared to the CVD method, especially for the low-melting-temperature glass substrates preferred for display applications.

3.2. Electrophoretic Deposition. Electrophoretic deposition (EPD) is a high-throughput process[49,50] for production of films/coating with good homogeneity and packing density. It can be applied to essentially any solid with small particle sizes or a colloidal suspension.[50] We have shown recently that preformed CNTs can be deposited on various surfaces with controlled thickness and morphology via EPD.[51]

The first step in this process is to stabilize a suspension of CNTs in a suitable solvent, which is challenging for CNTs. Although surfactants can be used, they are difficult to remove completely after deposition. The residual surfactants can seriously affect the performances of the nanotubes.[51] DMF, a commonly used surfactant, interacts strongly with the CNTs. IR spectroscopy studies of SWNT films deposited from a SWNT/DMF suspension show strong DMF signals even after vacuum annealing.[51] A very dilute suspension of SWNTs in alcohol (i.e., 1 mg of SWNT in 200 mL of ethanol) is typically used. A small amount of "charger" such as $MgCl_2$ is added to the suspension. Upon application of a direct current electrical field between the substrate and a counter electrode, the SWNTs migrate toward the substrate. The migration direction is controlled by the charger added. The film of long SWNTs is porous, with clearly resolved SWNT bundles, while the

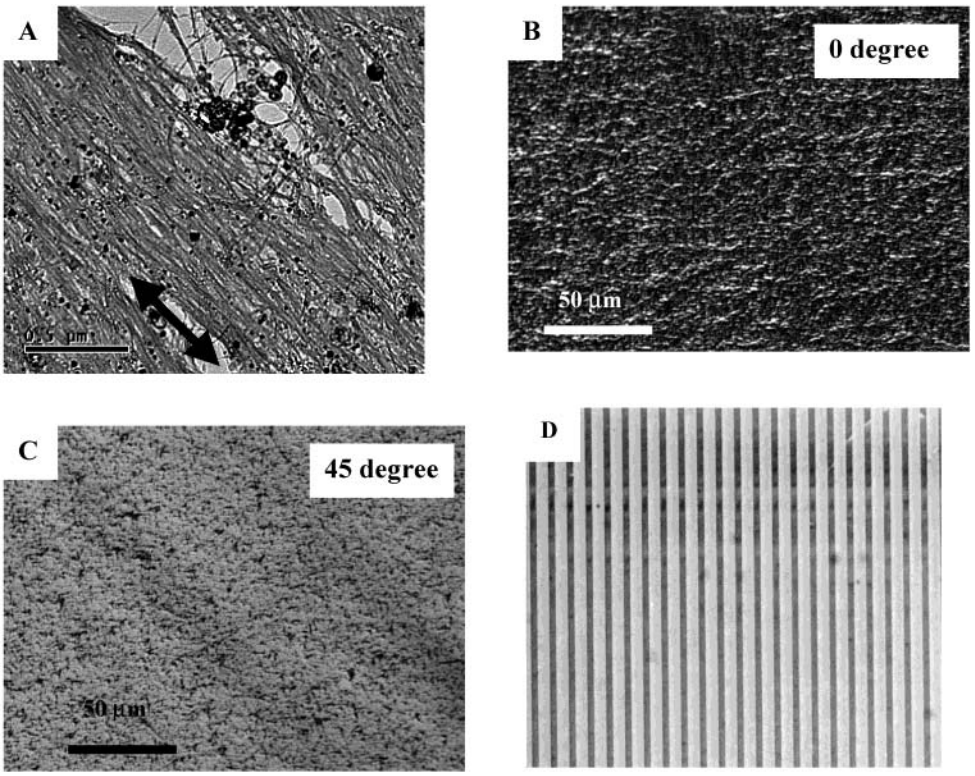

FIGURE 8. (A) TEM image of a self-assembled SWNT membrane. The membranes are only a few bundles thick. (B,C) Polarized optical microscope images of a thick SWNT film, taken using a white incident light and a pair of cross-polar polarizer and analyzer. The nanotube alignment direction was 0° (B) and 45° (C) with respect to the polarizer. (D) Patterned SWNT structures formed by the self-assembly process. The nanotube stripes (dark color region) are 100 μm in width.

film of short SWNTs has a much higher packing density. The deposition rate depended on several factors, including the concentration of the SWNT suspension, the charger concentration, and the current. Beyond fabrication of uniform CNT films/coating, the EPD technique can be used to deposit CNTs onto more complicated structures. This can be realized by either using a mask or taking advantage of the fact that deposition occurs only on the conducting surfaces.

4. Electron Field Emission Properties

Electron field emission is a quantum process where, under a sufficiently high external electrical field, electrons can escape from the metal surface to the vacuum level by tunneling.[52] Compared to thermionic emission, this is a preferred mechanism to extract electrons because no heating is required and the emission current can be controlled by the external field. The basic physics of field emission is summarized by the Fowler−Nordheim equation, which states that the emission current increases exponentially with increasing electrical field.[53] For a metal with a flat surface, the threshold field is typically around 10^4 V/μm, which is impractically high. All the field emission materials reply on field enhancement at the sharp tips/protrusions. The typical threshold fields are in the order of 10−100 V/μm for 10 mA/cm^2 current density (Table 1).

Carbon nanotubes have atomically sharp tips and large aspect ratios (>10^3) and, as a result, much larger field

Table 1. Electron Field Emission Characteristics of Typical Emissive Materials

cathode material	threshold field (V/μm) for a current density of 10 mA/cm^2
Mo tips	50−100
Si tips	50−100
p-type diamond	160
defective CVD diamond	30−120
amorphous diamond	20−40
cesium-coated diamond	20−30
graphite powders	10−20
nano-diamond	3−5 (unstable >30 mA/cm^2)
carbon nanotubes	2−5 (stable >1 μA/tube)

enhancement factors than the conventional emitters, such as the Spindt-type tips. Experiments have shown that the emission turn-on field of CNTs is 1−2 V/μm,[54−57] significantly lower than the values reported for other electron-emissive materials (Table 1). Compared to diamond emitters, the CNTs are much more stable at high currents. A stable emission current of >1 μA has been observed from an individual SWNT.[58] These properties make the CNTs attractive for technological applications. Indeed, the potential of using CNTs as cold cathodes has been demonstrated in devices such as field emission flat panel displays (FEDs),[59] lighting elements,[60] and discharge tubes for over-voltage protection.[61]

Most of the cold-cathode applications require a significantly higher emission current than that which can be delivered from a single CNT. For example, FED requires a current density of 1−10 mA/cm^2,[62] while other applications, such as microwave amplifiers, demand a much higher output.[63] For these applications, macroscopic CNT

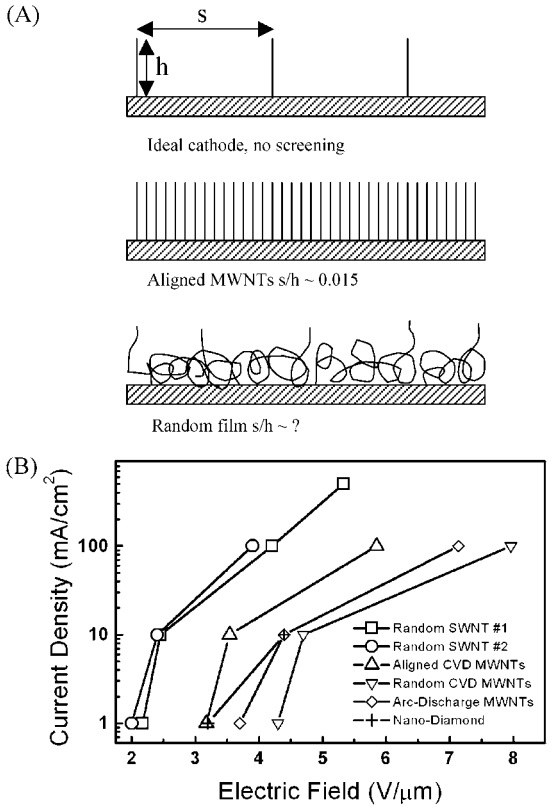

FIGURE 9. (A) Schematics illustrating the different geometries of macroscopic CNT field emission cathodes. In the ideal case (top), the CNTs are aligned in the field direction and well-spaced (S/H > 1) so that there is no electrical screening. (B) Experimentally measured electron emission threshold fields of different types of carbon nanotubes.

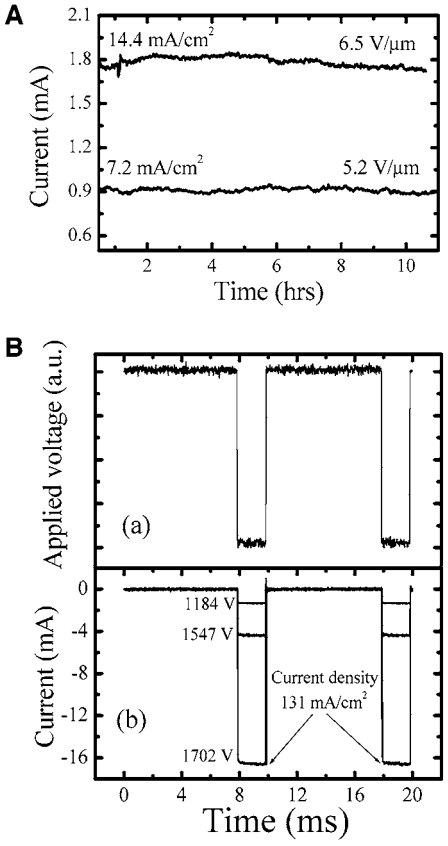

FIGURE 10. (A) Emission stability of the SWNT film continuously operated in a direct current mode without feedback. (B) Pulsed emission current. The total current of 16 mA can be obtained from 4-mm-diameter sample at an electric field of 11.3 V/μm.

cathodes are required. Although an individual CNT can deliver an extremely high and stable emission current,[58] the current density and stability decrease drastically as the cathode area increases. For macroscopic cathodes, the emission characteristics depend not only on the structure of *individual* nanotubes/bundles but also on their higher level architectures. For example, the emission site density is closely related to the uniformity and density of CNTs.[64] A low emission site density of 10^3-10^4 site/cm^2 means that, even at 1 mA/cm^2, the current extracted from each CNT is close to the limit. In the ideal case, one would like to have a cathode with well-spaced CNTs aligned in the electrical field direction (Figure 9A). Although aligned MWNT-like structures can now be fabricated by a variety of CVD mehods, these materials are highly defective. In most cases, the spacing between the individual MWNTs cannot be controlled. We compared the emission properties of CNTs with different structure and morphology.[65] The results (Figure 9B) show that the emission threshold fields of all the CNT materials are comparable within a factor of 2−3, regardless of the orientation and structure. However, SWNTs fabricated by the laser ablation method are more stable at the high current densities.

Here we show the emission characteristics of macroscopic SWNT cathodes after optimizing the CNT density, uniformity, and adhesion. The data were collected using the parallel-plate geometry. Figure 10A shows the emission stability of a SWNT cathode. Under a constant voltage without feedback, no overall decay in the emission current is observed over a 10-h period at a total current of 1.8 mA(14 mA/cm^2). The standard deviation of current fluctuation is 2−3%. By incorporation of a simple feedback loop,[15] the fluctuation can be further reduced to below 1%. Figure 10B shows the pulse emission currents triggered by various pulsed voltages. The emission current can be readily controlled by the input voltage signal. No delay between the applied voltage and the onset of the emission current was observed. A total emission current of 16 mA was obtained from a 4-mm-diameter cathode at an 11.3 V/μm electric field (the current output is presently limited by the power supply used). The high emission current and current density of these cathodes make them attractive for a variety of vacuum electronic devices.

We thank our colleagues at the North Carolina Center for Nanoscale Materials, in particular J. Liu, J. P. Lu, L. McNeil, S. Washburn, and Y. Wu, for discussion and collaboration. O.Z. thanks current and former students, postdocs, and visitors for their contribution to this work and is grateful for financial support from an ONR MURI program and grants from NASA and NSF.

References

(1) Kroto, H. W.; Heath, J. R.; O'Brien, S. C.; Curl, R. F.; Smalley, R. E. C_{60} Buckminsterfullerene. *Nature* **1985**, *315*, 162.

(2) Kratschmer, W.; Lamb, L. D.; Fostiropoulos, K.; Huffman, D. R. Solid C_{60}: a new form of carbon. *Nature* **1990**, *347*, 354.
(3) Iijima, S. Helical Microtubules of Graphitic Carbon. *Nature* **1991**, *354*, 56−58.
(4) Hebard, A. F.; Rosseinsky, M. J.; Haddon, R. C.; Murphy, D. W.; Glarum, S. H.; Palstra, T.; Ramirez, A. P.; Kortan, A. R. Superconductivity of 18K in potassium-doped C_{60}. *Nature* **1991**, *350*, 600.
(5) Ajayan, P. M.; Zhou, O. Applications of Carbon Nanotubes. In *Carbon Nanotubes: Synthesis, Structure, Properties, and Applications*; Dresselhaus, M. S., Dresselhaus, G., Avouris, P., Eds.; Topics in Applied Physics 80; Springer-Verlag: Heidelberg, 2000; pp 391−425.
(6) Special Issue on Buckministerfullerenes. *Acc. Chem. Res.* **1992**, *25* (3).
(7) Kroto, H. W., Fischer, J. E., Cox, D. E., Eds. *The Fullerenes*; Pergamon Press Ltd.: Oxford, 1993.
(8) Ebbesen, T. W.; Ajayan, P. M. Large-scale synthesis of carbon nanotubes. *Nature* **1992**, *358*, 16.
(9) Journet, C.; Maser, W. K.; Bernier, P.; Loiseau, A.; Chapelle, M. L. d. l.; Lefrant, S.; Deniard, P.; Lee, R.; Fischer, J. E. Large Scale Production of Single Wall Carbon Nanotubes by the Electric Arc Technique. *Nature* **1997**, *388*, 756−758.
(10) Thess, A.; Lee, R.; Nikdaev, P.; Dai, H.; Petit, P.; Robert, J.; Xu, C.; Lee, Y. H.; Kim, S. G.; Rinzler, A. G.; Colbert, D. T.; Scuseria, G. E.; Tomanek, D.; Fischer, J. E.; Smalley, R. E. Crystalline Ropes of Metallic Carbon Nanotubes. *Science* **1996**, *273*, 483−487.
(11) Ren, Z. F.; Huang, Z. P.; Xu, J. W.; Wang, J. H.; Bush, P.; Siegal, M. P.; Provencio, P. N. Synthesis of large Arrays of Well-Aligned Carbon Nanotubes on Glass. *Science* **1998**, *282*, 1105.
(12) Fan, S.; Chapline, M. G.; Franklin, N. R.; Tombler, T. W.; Cassell, A. M.; Dai, H. Self-Oriented Regular Arrays of Carbon Nanotubes and Their Field Emission Properties. *Science* **1999**, *283*, 512−514.
(13) Bower, C.; Zhou, O.; Zhu, W.; Werder, D. J.; Jin, S. Nucleation and growth of carbon nanotubes by microwave plasma chemical vapor deposition. *Appl. Phys. Lett.* **2000**, *77* (17), 2767−2769.
(14) Su, M.; Zheng, B.; Liu, J. A scalable CVD method for the synthesis of single-walled carbon nanotubes with high catalyst productivity. *Chem. Phys. Lett.* **2000**, *322*, 321−326.
(15) Bandow, S.; Asaka, S.; Saito, Y.; Rao, A. M.; Grigorian, L.; Richter, E.; Ecklund, P. C. Effect of the growth temperature on the diameter distribution and chirality of single-wall carbon nanotubes. *Phys. Rev. Lett.* **1998**, *80* (17), 3779−3782.
(16) Yudasaka, M.; Komatsu, T.; Ichihashi, T.; Achiba, Y.; Iijima, S. Pressure dependence of the structures of carbonaceous deposits formed by laser ablation on targets composed of carbon, nickel, and cobalt. *J. Phys. Chem. B* **1998**, *102*, 4892−4896.
(17) Bower, C.; Suzuki, S.; Tanigaki, K.; Zhou, O. Synthesis and Structure of Pristine and Cesium Intercalated Single-Walled Carbon Nanotubes. *Appl. Phys.* **1998**, *A67*, 47−52.
(18) Katauta, H.; Kumazawa, Y.; Maniwa, Y.; Umezu, I.; Suzuki, S.; Ohtsuka, Y.; Achiba, Y. Optical properties of single-wall carbon nanotubes. *Synth. Met.* **1999**, *103*, 2555−2558.
(19) Tang, X. P.; Kleinhammes, A.; Shimoda, H.; Fleming, L.; Bower, C.; Sinha, S.; Zhou, O.; Wu, Y. Electronic structures of single-walled carbon nanotubes determined by NMR. *Science* **2000**, *228*, 492−494.
(20) Odom, T. W.; Huang, J. L.; Kim, P.; Lieber, C. M. Atomic Structure and Electronic Properties of Single-Walled Carbon Nanotubes. *Nature* **1998**, *391*, 62−64.
(21) Qin, L.-C.; Iijima, S.; Kataura, H.; Maniwa, Y.; Suzuki, S.; Achiba, Y. Helicity and Packing of Single-Walled Carbon Nanotubes Studied by Electron Nanodiffraction. *Chem. Phys. Lett.* **1997**, *268*, 101−106.
(22) Tang, X.-P.; Kleinhammes, A.; Shimoda, H.; Fleming, L.; Bennoune, K. Y.; Bower, C.; Zhou, O.; Wu, Y. Electronic Structures of Single-Walled Carbon Nanotubes Studied by NMR. *Mater. Res. Soc. Symp. Proc.* **1999**, *593*, 143−148.
(23) Yildirim, T.; Zhou, O.; Fischer, J. E. In *The Physics of Fullerene-Based and Fullerene-Related Materials*; Andreoni, W., Ed.; Kluwer: Dordrecht/Boston/London, 2000.
(24) Rao, A. M.; Richter, E.; Bandow, S.; Chase, B.; Ecklund, P. C.; Williams, K. A.; Fang, S.; Subbaswamy, K. R.; Menon, M.; Thess, A.; Smalley, R. E.; Dresselhaus, G.; Dresselhaus, M. S. Diameter-selective Raman scattering from vibrational modes in carbon nanotubes. *Science* **1997**, *275*, 187.
(25) Porter, D. A.; Easterling, K. E. *Phase transformation in metals and metal alloys*; Van Nostrand Reinhold: New York, 1981.
(26) Shelimov, K. B.; Esenaliev, R. O.; Rinzler, A. G.; Huffman, C. B.; Smalley, R. E. Purification of single-wall carbon nanotubes by ultrasonically assisted filtration. *Chem. Phys. Lett.* **1998**, *282*, 429−434.
(27) Ebbesen, T. W.; Ajayan, P. M.; Hiura, H.; Tanigaki, K. Purification of nanotubes. *Nature* **1994**, *367* (10), 519.
(28) Tohji, K.; Goto, T.; Takahashi, H.; Shinoda, Y.; Shimizu, N.; Jeyadevan, B.; Matsuoka, I.; Saito, Y.; Kasuya, A.; Ohsuna, T.; Hiraga, K.; Nishina, Y. Purifying Single-Walled Nanotubes. *Nature* **1996**, *383*, 679.
(29) Monthioux, M.; Smith, B. W.; Burteaux, B.; Claye, A.; Fischer, J. E.; Luzzi, D. E. Sensitivity of single-wall carbon nanotubes to chemical processing: an electron microscopy investigation. *Carbon* **2001**, *39*, 1251−1272.
(30) Zhou, O.; Gao, B.; Bower, C.; Fleming, L.; Shimoda, H. Structure and electrochemical properties of carbon nanotube intercalation compounds. *Mol. Cryst. Liq. Cryst.* **2000**, *340*, 541−546.
(31) Gao, B.; Bower, C.; Lorentze, J.; Fleming, L.; Kleinhammes, A.; Tang, X. P.; McNeil, L. E.; Wu, Y.; Zhou, O. Enhanced Saturation Li Composition in Ball-Milled Single-Walled Carbon Nanotubes. *Chem. Phys. Lett.* **2000**, *327*, 69−75.
(32) Pierard, N.; Fonseca, A.; Konya, Z.; Willems, I.; Van Tendeloo, G.; Nagy, J. B. Production of short carbon nanotubes with open tips by ball milling. *Chem. Phys. Lett.* **2001**, *335*, 1.
(33) Stepanek, I.; Maurin, G.; Bernier, P.; Gavillet, J.; Loiseau, A.; Edwards, R.; Jaschinski, O. Nano-mechanical cutting and opening of single wall carbon nanotubes. *Chem. Phys. Lett.* **2000**, *331*, 125.
(34) Ajayan, P. M.; Ebbesen, T. W.; Ichihashi, T.; Iijima, S.; Tanigaki, K.; Hiura, H. Opening carbon nanotubes with oxygen and implications for filling. *Nature* **1993**, *362*, 522.
(35) Liu, J.; Rinzler, A.; Dai, H.; Hafner, J.; Bradley, A. R.; Boul, P.; Lu, A.; Iverson, T.; Shelimov, A. K.; Huffman, C.; Rodriguez-Macias, F.; Shon, Y.; Lee, R.; Colbert, D.; Smalley, R. E. Fullerene Pipes. *Science* **1998**, *280*, 1253−1256.
(36) Shimoda, H.; Gao, B.; Tang, X. P.; Kleinhammes, A.; Fleming, L.; Wu, Y.; Zhou, O. Lithium intercalation into opened single wall carbon nanotubes: storage capacity and electronic properties. *Phys. Rev. Lett.* **2002**, *88* (1), 015502.
(37) Claye, A.; Fischer, J. E.; Huffmand, C. B.; Rinzler, A. G.; Smalley, R. E. Solid-state electrochemistry of the Li single wall carbon nanotube system. *J. Electrochem. Soc.* **2000**, *147* (8), 2845−2852.
(38) Suzuki, S.; Bower, C.; Zhou, O. In-situ TEM and EELS Observations of Alkali Metal Intercalation with SWNT Bundles. *Chem. Phys. Lett.* **1998**, *285*, 230−234.
(39) Gao, B.; Shimoda, H.; Tang, X. P.; Kleinhammes, A.; Fleming, L.; Wu, Y.; Zhou, O. Lithium storage in single-wall carbon nanotubes. In *Nanonetwork Materials: Fullerenes, Nanotubes, and Related Systems*, Proceedings of the International Symposium on Nanonetwork Materials, Kamakura, Japan, 15−18 January 2001; Saito, S., et al., Eds.; AIP: Melville, NY, 2001; Vol. 590, pp 95−99.
(40) Zhou, O.; Fleming, R. M.; Murphy, D. W.; Chen, C. T.; Haddon, R. C.; Ramirez, A. P.; Glarum, S. H. Defects in Carbon Nanotubes. *Science* **1994**, *263*, 1744−1747.
(41) Lee, R. S.; Kim, H. J.; Fischer, J. E.; Thess, A.; Smalley, R. E. Conductivity enhancement in single-walled carbon nanotube bundles doped with K and Br. *Nature* **1997**, *388*, 255−257.
(42) Rao, A. M.; Eklund, P. C.; Bandow, S.; Thess, A.; Smalley, R. E. Raman Scattering Study of Charge Transfer in Doped Carbon Nanotube Bundles. *Nature* **1997**, *388*, 257−259.
(43) Grigorian, L.; Williams, K. A.; Fang, S.; Sumanasekera, G. U.; Loper, A. L.; Dickey, E. C.; Pennycook, S. J.; Eklund, P. C. Reversible intercalation of charged iodine chains into carbon nanotube ropes. *Phys. Rev. Lett.* **1998**, *80*, 5560−5563.
(44) Suzuki, S.; Bower, C.; Kiyokura, T.; Nath, K. G.; Watanabe, Y.; Zhou, O. Photoemission spectroscopy of single-walled carbon nanotube bundles. *J. Electron Spectrosc.* **2001**, *114−116*, 225−228.
(45) Suzuki, S.; Bower, C.; Watanabe, Y.; Zhou, O. Work functions and valence band states of pristine and Cs-intercalated single-walled carbon nanotube bundles. *Appl. Phys. Lett.* **2000**, *76* (26), 4007−4009.
(46) Wadhawan, A.; Stallcup, R. E.; Perez, J. M. Effects of Cs deposition on the field-emission properties of single-walled carbon nanotube bundles. *Appl. Phys. Lett.* **2001**, *78* (1), 108−110.
(47) Ulman, A. *An Introduction to Ultrathin Organic Films: From Langmuir−Blodgett to Self-Assembly*; Academic Press: Boston, 1991.
(48) Shimoda, H.; Oh, S. J.; Geng, H. Z.; Walker, R. J.; Zhang, X. B.; McNeil, L. E.; Zhou, O. Self-assembly of carbon nanotubes. *Adv. Mater.* **2002**, *14* (12), 899−901.
(49) Pohl, H. A. *Dielectrophoresis*; Cambridge University Press: Cambridge, UK, 1978.
(50) Van der Biest, O.; Vandeperre, L. J. Electrophoretic deposition of materials. *Annu. Rev. Mater. Sci.* **1999**, *29*, 327.
(51) Gao, B.; Yue, G. Z.; Qiu, Q.; Cheng, Y.; Shimoda, H.; Fleming, L.; Zhou, O. Fabrication and electron field emission properties of carbon nanotube films by electrophoretic deposition. *Adv. Mater.* **2001**, *13* (23), 1770−1774.

(52) Gomer, R. *Field Emission and Field Ionization*; Harvard University Press: Cambridge, MA, 1961,
(53) Brodie, I.; Spindt, C. A. Vacuum Microelectronics. *Adv. Electron. Electron Phys.* **1992**, *83*, 1−106.
(54) Heer, W. A. d.; Chatelain, A.; Ugarte, D. A Carbon Nanotube Field-Emission Electron Source. *Science* **1995**, *270*, 1179−1180.
(55) Collins, P. G.; Zettl, A. A Simple and Robust Electron Beam Source From Carbon Nanotubes. *Appl. Phys. Lett.* **1996**, *69* (13), 1969−1971.
(56) Bonnard, J. M.; Salvetat, J. P.; Stockli, T.; Herr, W. A. d.; Forro, L.; Chatelain, A. Field emission from single-wall carbon nanotube films. *Appl. Phys. Lett.* **1998**, *73* (7), 918−920.
(57) Zhu, W.; Bower, C.; Zhou, O.; Kochanski, G. P.; Jin, S. Very high current density from carbon nanotube field emitters. *Appl. Phys. Lett.* **1999**, *75* (6), 873−875.
(58) Dean, K. A.; Chalamala, B. R. Current saturation mechanisms in carbon nanotube field emitters. *Appl. Phys. Lett.* **2000**, *76*, 375.
(59) Choi, W. B.; Chung, D. S.; Kang, J. H.; Kim, H. Y.; Jin, Y. W.; Han, I. T.; Lee, Y. H.; Jung, J. E.; Lee, N. S.; Park, G. S.; Kim, J. M. Fully sealed, high-brightness carbon-nanotube field-emission display. *Appl. Phys. Lett.* **1999**, *75*, 3129.
(60) Saito, Y.; Uemura, S.; Hamaguchi, K. Cathode Ray Tube Lighting Elements with Carbon Nanotube Field Emitters. *Jpn. J. Appl. Phys.* **1998**, *37*, L346−L348.
(61) Rosen, R.; Simendinger, W.; Debbault, C.; Shimoda, H.; Fleming, L.; Stoner, B.; Zhou, O. Application of carbon nanotubes as electrodes in gas discharge tubes. *Appl. Phys. Lett.* **2000**, *76* (13), 1197−1199.
(62) Castellano, J. A. *Handbook of Display Technology*; Academic Press: San Diego, 1992.
(63) Scott, A. W. *Understanding Microwaves*; John Wiley & Sons: New York, 1993.
(64) Bonnard, J.-M.; Weiss, N.; Kind, H.; Stockli, T.; Forro, L.; Kern, K.; Chatelain, A. Tuning the electron emission properties of patterned carbon nanotube films. *Adv. Mater.* **2001**, *13* (3), 184−188.
(65) Bower, C.; Zhou, O.; Zhu, W.; Ramirez, A. G.; Kochanski, G. P.; Jin, S. Fabrication and field emission properties of carbon nanotube cathodes. In *Amorphous and Nanostructured Carbon*; Sullivan, J. P., et al., Eds.; Materials Research Society Symposium Proceedings 593; Materials Research Society: Warrendale, PA, 2000; p 215.

AR010162F